Noname manuscript No.
(will be inserted by the editor)

The wrinkling of a twisted ribbon

Robert V. Kohn · Ethan O'Brien

Received: date / Accepted: date

Abstract Recent experiments by Chopin and Kudrolli [PRL 111:174302, 2013] showed that a thin elastic ribbon, when twisted into a helicoid, may wrinkle in the center. We study this from the perspective of elastic energy minimization, building on recent work by Chopin, Démery, and Davidovitch [J Elasticity 119, 2015, 137-189] in which they derive a modified von Kármán functional and solve the relaxed problem. Our main contribution is to show matching upper and lower bounds for the minimum energy in the small-thickness limit. Along the way, we show that the displacements must be small where we expect that the ribbon is helicoidal, and we estimate the wavelength of the wrinkles.

1 Introduction

Consider a thin elastic ribbon, clamped firmly on both ends and twisted into a helicoid, as seen in Figure 1. A flat sheet is not related to a helicoid by an isometry, so we need to apply some force on the clamps in order to maintain the helicoidal shape. It is a curious fact that, for not too extreme values of the force, the ribbon develops small-scale wrinkles down the center, perpendicular to the axis of rotation. In fact, a twisted ribbon exhibits a range of morphologies: for example, if stretched with small enough force the ribbon forms triangular facets separated by creases, and with large enough force it might not wrinkle at all. In the present work we focus on the wrinkled ribbon regime.

We approach this system from the perspective of elastic energy minimization. The starting point of our analysis is a small-slope, small-displacement elastic en-

Robert V. Kohn
Courant Institute of Mathematical Sciences, New York University, New York, NY 10012, USA.
E-mail: kohn@cims.nyu.edu

Ethan O'Brien
Courant Institute of Mathematical Sciences, New York University, New York, NY 10012, USA.
E-mail: obrien@cims.nyu.edu

This work was partially supported by the National Science Foundation through grants OISE-0967140 and DMS-1311833.

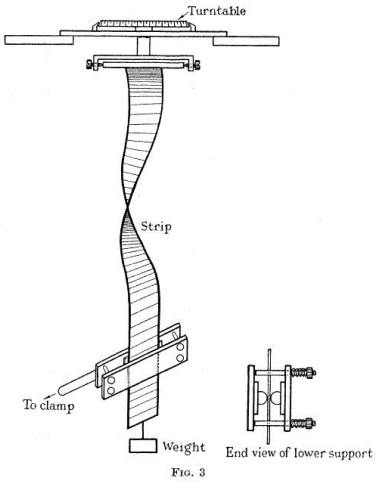

Fig. 1: A. E. Green's sketch of a twisted steel ribbon. First appeared in [19]; now in the public domain.

ergy functional (Equation 2), which is reminiscent of von Kármán plate theory. In Theorem 1 we prove matching upper and lower bounds for the minimum energy in the regime where the non-dimensional thickness h is small. Of course, to prove an upper bound it suffices to find an ansatz that achieves the desired energy scaling, but to find a lower bound we need to use an ansatz-free argument.

The idea that we can study pattern formation by proving upper and lower bounds on an energy functional with a small parameter is not new; see, for instance, [21] for an overview. Similarly, the study of wrinkling as an example of energy-driven pattern formation has provoked recent interest in both the physics and mathematics literature. A general feature of these problems is that wrinkling arises as an energetically preferable alternative to compression [2]. There seem to be two broad categories: "tensile wrinkling" and "compressive wrinkling." The former arises when there is tension in one direction and compression in the other; the tension determines the direction of the wrinkling, and induces an energetic preference for small-amplitude wrinkling, see e.g. [9]. In compressive wrinkling, on the other hand, the wrinkles serve to avoid biaxial compression; examples include the herringbone pattern seen in a compressed thin film on a compliant substrate (see e.g. [22] and other work cited therein) and the configuration adopted by a compressed thin film when it blisters from its substrate (see e.g. [20] [8], as well as [4] and other work cited therein). In the compressive setting the wrinkling patterns are often not very regular; local minima of the elastic energy can be very important; and folds or other types of singularities can occur instead of wrinkling [30].

A growing literature is developing concerning the "scaling law of the elastic energy" – i.e. its dependence on sheet thickness – for problems involving wrinkling. The point is that the scaling law is closely related to the character of the wrinkling. This viewpoint has been especially fruitful in tensile problems, where the overall direction of the wrinkling is not in doubt. It has also been explored in

Fig. 2: Twisted mylar ribbons: experimental results from [11]. Used with permission.
Top: a wrinkled helicoid.
Bottom: a creased helicoid.

some compressive problems, for example compressed thin film blisters [20] [4] and the herringbone pattern [22]. However, in other compressive settings the spatial complexity seen in experiments is not associated with a scaling law, but rather with local minima, defects, or history, see e.g. [17].

The problem considered in this paper lies more or less at the boundary between the "tensile" and "compressive" regimes. Indeed, there is no tension in the wrinkled zone to set the direction of the wrinkles. But the *outer part* of our twisted ribbon is in tension, and as a result its configuration is more or less fixed. The rigidity of the outer part permits us to analyze the wrinkling of the inner part using methods reminiscent of the tensile setting. Our lower bound on the elastic energy draws inspiration from a recent paper on metric-driven wrinkling [5]. We note, however, that the rigidity of the outer part was as assumption in [5], whereas it something we prove in the present setting.

We remark that besides analysis of the energy scaling law, there are also other approaches to understanding the local length scale of wrinkling. In particular, important progress has recently been achieved using a more ansatz-based approach [27][23], for problems where the macroscopic curvature of the deformed shape plays an important role.

1.1 Experimental results

There are at least two sets of experiments on the wrinkling of a twisted ribbon; first in 1936 with steel ribbons [19], and recently with mylar ribbons [11]. Both experiments clamped the ribbon firmly on both ends, twisted it into a helicoid, and pulled on the clamps with prescribed force F. For any value of $F > 0$ the outer edges are stretched vertically (that is, in the direction of the axis of rotation). For small enough F the center would be compressed if the ribbon were a helicoid. We define a 'critical force' F_{crit}, which determines whether or not the ribbon is wrinkled; it is the smallest F such that the helicoid is not under compression anywhere. In this article we are interested in the regime $0 < F < F_{\mathrm{crit}}$. The zones which would be compressed, if the ribbon were helicoidal, wrinkle instead.

We briefly discuss some of the possible morphologies of a twisted ribbon found in [11] (see Figure 2). If the clamps on the ends of the ribbon are pushed too close together then there is no reason for the ribbon to be under tension anywhere ($F =$

0), and we have no reason to think that such a deformation is helicoidal. In fact, the ribbon looks as though it wraps around an imaginary cylinder. Alternatively, if the clamps are too far apart ($F > F_{\text{crit}}$) then the entire ribbon is under tension. In practice we see either no wrinkles or, if F is very large, 'transverse buckling'. We do not have a definitive physical explanation of transverse buckling.[1]

For small enough force, Chopin and Kudrolli observed that the mylar ribbon did not wrinkle [11]. Instead, it formed flat, triangular facets separated by creases, as shown in Figure 2. Informally, we expect that the triangular facets are found in the regime $0 < F \ll F_{\text{crit}}$; meaning that to explain the creased ribbon one should consider at least *two* small parameters; the thickness h and the force F. A recent paper modeling this is [24].

1.2 Connections to previous work on the twisted ribbon

Green analyzed the wrinkling of his steel ribbons as a bifurcation from the unwrinkled state [19]. Chopin et al. used a quite different approach: they studied the minimizer of a relaxed energy [10].[2] These two techniques differ dramatically in both the level of detail of their results and their range of validity. The bifurcation theory approach provides detailed information about the length scale of wrinkling, but it is only applicable when the sheet thickness is sufficiently large (so F is close to F_{crit}). Minimization of the relaxed energy is appropriate in the opposite "far from threshold" limit, when the thickness is sufficiently small (so F is well below F_{crit} and a bifurcation-based analysis would have to look deep in the bifurcation diagram). However the relaxed energy does not provide information about the length scale of wrinkling; as a result, the analysis of Chopin et al. involves mainly the macroscopic shape of the ribbon and the extent of the wrinkled zone.

1.3 A summary of the main result

Our approach follows [10]. We seek to minimize the same elastic energy functional, called $E^{(h)}$ and described in Equation (2), as the thickness h vanishes. In Theorem 1 we show that the excess energy due to positive h scales as $h^{4/3}$: there are constants C, C' such that

$$\mathcal{E}_0 + Ch^{4/3} \leq \min E^{(h)} \leq \mathcal{E}_0 + C'h^{4/3}. \tag{1}$$

Before discussing the significance of Equation (1), we first describe the structure of $E^{(h)}$. The energy $E^{(h)}$ is taken to be a sum of two terms: the *membrane* (or *stretching*) energy and the *bending* energy. It is intuitively clear that the bending energy is small in h: stretching a thin sheet ought to take much more energy than bending it. On the other hand, the membrane energy alone is non-convex

[1] There are at least two candidates. Firstly, this buckling may be related to the Poisson ratio-driven wrinkling of a stretched but untwisted sheet, as analyzed by Cerda and Mahadevan [9]. Alternatively, these could have to do with the fact that, using a nonlinear energy functional such as Equation (5), the helicoid is *not* the relaxed solution. Our model sees neither effect: we exclude the first by assuming Poisson ratio 0, and the second by using a small-displacement, small-slope energy functional.

[2] This is called tension field theory in the physics literature.

(more generally, not quasiconvex), so if we ignore the bending energy then there might not exist a minimizer. The bending energy is convex in the highest-order derivatives present, so $E^{(h)}$ has a minimizer for any $h > 0$.[3]

Chopin et al. [10] identified the constant $\mathcal{E}_0$ in Equation (1) by minimizing the relaxed energy $E^{(0)}$ (we do something similar in Section 2.3). In an appropriate topology the minimizers of $E^{(h)}$ tend (up to a subsequence) to a minimizer of $E^{(0)}$ as h tends to 0. Thus minimizing $E^{(0)}$ gives partial information about the minimizers of $E^{(h)}$, which are the objects of interest. This information is important but incomplete: any features that vanish in the limit $h \to 0$ are invisible to the relaxed problem. For instance, it is natural to ask about the wavelength or amplitude of the wrinkles, and minimizing the relaxed energy cannot easily estimate either of those quantities. We prove energy scaling laws such as Equation (1) to find more quantitative bounds (in an L^p sense). For example, in the proof of Proposition 4 we show that the wrinkles should have amplitude of at most order $(\min E^{(h)} - \mathcal{E}_0)^{1/4}$ in L^2 (Equation 22). The energy scaling law shows us that the wrinkles in fact have amplitude of at most $h^{1/3}$.

2 The energy of a twisted ribbon

We will work with a small-displacement, small-slope energy functional, which is reminiscent of but not identical to the von Kármán energy. Additionally, we consider only isotropic materials with Poisson ratio 0. The key idea is that whereas von Kármán plate theory considers small-slope deformations of a flat plate, our analysis considers deformations of the strip whose image is a small-slope perturbation of a helicoid. Recall that in von Kármán plate theory the elastic energy depends on an in-plane displacement $\boldsymbol{u}$ and an out-of-plane displacement v; in our setting, the analogous objects are the *tangential displacement* $\boldsymbol{u}$ and the *normal displacement* v.

2.1 An elastic energy functional for a twisted ribbon

We start by making the verbal description of the energy in Section 1 somewhat more precise. We consider an energy functional of the form

$$E^{(h)} = \int_\Omega |\mathbf{M}(\boldsymbol{x})|^2 + h^2 |\mathbf{B}(\boldsymbol{x})|^2 \, \mathrm{d}\boldsymbol{x},$$

where $\mathbf{M}$ and $\mathbf{B}$ are symmetric tensors. The physical interpretation is that, if $\boldsymbol{a}$ is a unit vector, $\langle \boldsymbol{a}, \mathbf{M}(\boldsymbol{x})\boldsymbol{a}\rangle$ (respectively, $\langle \boldsymbol{a}, \mathbf{B}(\boldsymbol{x})\boldsymbol{a}\rangle$) determine the amount of stretching (respectively, bending) at a point $\boldsymbol{x}$ and in the direction of $\boldsymbol{a}$. The Frobenius norms $|\mathbf{M}|^2$ and $|\mathbf{B}|^2$ are reasonable, but by no means canonical, measures of the total amount of bending or stretching at a point. Physically, we have assumed that the material is isotropic and has Poisson ratio 0.

The ribbon's energy is given by

$$E^{(h)}(\boldsymbol{u}, v) = \int_\Omega |\mathbf{M}(\boldsymbol{u}, v)|^2 + h^2 \, |\mathbf{B}(v)|^2 \, \mathrm{d}\boldsymbol{x} \tag{2}$$

[3] Note the similarity to Landau theories: a small but convex term regularizes a non-convex minimization problem.

where

$$\mathbf{M} = \mathrm{e}(\boldsymbol{u}) + \frac{1}{2}\begin{pmatrix} \partial_1 v \\ \partial_2 v + \omega x_1 \end{pmatrix}^{\otimes 2} - \frac{1}{2}\begin{pmatrix} 0 & \omega v \\ \omega v & \omega^2 \xi^2 \end{pmatrix}, \tag{3}$$

$$\mathbf{B} = \nabla\nabla v + \begin{pmatrix} 0 & \omega \\ \omega & 0 \end{pmatrix}, \text{ and} \tag{4}$$

$$\Omega = \left(-\frac{1}{2}, \frac{1}{2}\right) \times (0, l).$$

The ribbon is twisted by an amount ω around the x_2 axis, and allowed to compress by an amount $\frac{1}{2}\omega^2\xi^2$. The tangential and normal displacements (from the twisted and slightly compressed state) are $\boldsymbol{u}$ and v, respectively. We will see that the ribbon should wrinkle for $|x_1| < \xi$ and be flat outside that region.

The tensors $\mathbf{M}$ (for membrane) and $\mathbf{B}$ (bending) have the standard physical meaning. We give a non-rigorous derivation in Section 2.2, but in order to convince the reader that this energy functional is reasonable, we check that several geometric properties of the helicoid are present.

- A helicoid has negative Gaussian curvature. With $v = 0$, the Gaussian curvature is $\det(\mathbf{B}) = -\omega^2$.
- A compressed helicoid is described by $\boldsymbol{u} = \mathbf{0}$, $v = 0$. This should (for small enough values of compression) stretch vertical lines on the outside of the ribbon and compress those on the inside. The membrane term is given by $\mathbf{M} = \frac{1}{2}\omega^2\left(x_1^2 - \xi^2\right)\boldsymbol{e}^{(2)} \otimes \boldsymbol{e}^{(2)}$, which has these properties.

The main result of this work, stated imprecisely in Section 1.3, follows.

Theorem 1 (Energy scaling for a twisted ribbon with small thickness) *For any $l > 0$, $\omega > 0$ and $\xi \in \left(0, \frac{1}{2}\right)$ there exist constants $\mathcal{E}_0$, C and C' such that for all $h^{1/3} \leq 2\pi l$,*

$$\mathcal{E}_0 + Ch^{4/3} < \min_{\boldsymbol{u},v} E^{(h)}(\boldsymbol{u}, v) < \mathcal{E}_0 + C'h^{4/3}$$

where the minimum is over the class

1. *$\boldsymbol{u} \in W^{1,2}(\Omega, \mathbb{R}^2)$ with $\boldsymbol{u}(x_1, 0) = \boldsymbol{u}(x_1, l) = \mathbf{0}$, and*
2. *$v \in W^{2,2}(\Omega, \mathbb{R}^2)$ with $v(x_1, 0) = v(x_1, l) = 0$.*

Remark 1 (Other asymptotic regimes) The functional $E^{(h)}$ of Equation (2) depends on the thickness h, twist ω, length l and size of the wrinkled zone ξ. We have nondimensionalized so that the remaining natural length scale, the width of the ribbon, is taken to be 1 (and all other lengths, including ω^{-1}, are dimensionless). In this work we focus our attention on small h, with all other parameters held constant. The regime where h and $\frac{1}{2} - \xi$ are simultaneously small is especially interesting, but beyond the scope of this work: instead of wrinkling, we believe that the ribbon can form flat faces connected by creases. See [24] for a physics paper discussing the creased ribbon.

For the sake of clarity we will bury the dependence on these parameters in constants in most of our results, but because we expect the dependence of the lower bound on parameters other than h to be useful in future work we will keep track of these parameters in the proof of Proposition 3. We will adopt the following

convention: the implicit constant in $a(\boldsymbol{u}, v) \lesssim b(\boldsymbol{u}, v)$ may depend on l, ω and ξ. The implicit constant in $a(\boldsymbol{u}, v) \lessapprox b(\boldsymbol{u}, v)$ may depend on only ω.

The energy depends on the twist in a trivial fashion: $E_\omega^{(h)}(\omega^2 \boldsymbol{u}, \omega v) = \omega^4 E_1^{(h/\omega)}(\boldsymbol{u}, v)$. Here $E_\omega^{(h)}$ is the energy $E^{(h)}$ found in Equation (2), but with the dependence on the rate of twist ω made explicit.

2.2 The derivation of the energy

The energy $E^{(h)}$ of Equation (2) is not standard. We briefly and informally describe its origin, following a procedure described verbally in [10]. We emphasize that the problem has already been non-dimensionalized: the width of the ribbon is 1, and all variables with units of length are interpreted as length per unit width.

For the sake of brevity we start with a specific nonlinear energy for an elastic sheet:

$$I^{(h)}(\boldsymbol{\varphi}) = \int_\Omega \left| \sqrt{\nabla \boldsymbol{\varphi}(\boldsymbol{x})^T \nabla \boldsymbol{\varphi}(\boldsymbol{x})} - \mathrm{Id} \right|^2 + h^2 \left| \mathrm{I\!I}_{\boldsymbol{\varphi}}(\boldsymbol{x}) \right|^2 \mathrm{d}\boldsymbol{x}, \tag{5}$$

where $\boldsymbol{\varphi} : \Omega \to \mathbb{R}^3$ represents the position (as opposed to the displacement) of the sheet, and $\mathrm{I\!I}_{\boldsymbol{\varphi}}$ is the second fundamental form of the surface defined by $\boldsymbol{\varphi}$. As in $E^{(h)}$, we call the first term the *membrane* energy and the second the *bending* energy, with the same interpretation. Our derivation does not depend critically on the exact form of the energy, but the behaviour for $\nabla \boldsymbol{\varphi}$ near SO(3) is important: we have assumed that the elastic stiffness tensor is isotropic and has Poisson ratio 0.

We pause to recall an informal derivation[4] of von Kármán's energy functional for an elastic plate. Define the displacements $\boldsymbol{u}$ and v by $\boldsymbol{\varphi}(\boldsymbol{x}) = (x_1 + u_1, x_2 + u_2, v)$, and assume that these have small slope. One can then write down the leading-order dependence of the membrane and bending terms on $\boldsymbol{u}$ and v, and discard the higher-order terms to find the von Kármán energy. It is important to note that we do not assume that $\boldsymbol{u}$ and v are the same order; for instance, the leading order part of the membrane term is $\mathrm{e}(\boldsymbol{u}) + \frac{1}{2} \nabla v \otimes \nabla v$.

We proceed with our derivation of Equation (2), which is similar in spirit to the derivation of the von Kármán plate theory outlined above. The key difference is that we expand around a twisted and slightly compressed helicoid rather than a flat sheet. We assume from the start that ω is a small parameter, and that v scales as ω, and that $\boldsymbol{u}$ scales as ω^2. Furthermore, we assume that the first and second derivatives of the displacements $\boldsymbol{u}$ and v scale in the same manner. The thickness h is also small, but we make no assumptions about the relative sizes of h and ω.

Let $\left\{ \boldsymbol{r}^1, \boldsymbol{r}^2, \boldsymbol{r}^3 \right\}$ be a positively oriented orthonormal frame of unit vectors that depend on x_2 through the following rules:

1. $\boldsymbol{r}^2$ is constant,
2. $\partial_2 \boldsymbol{r}^1 = \omega \boldsymbol{r}^3$, and
3. $\partial_2 \boldsymbol{r}^3 = -\omega \boldsymbol{r}^1$.

We consider the energy as a function of displacements from a slightly compressed helicoid, rather than absolute position. To this end, we define $\boldsymbol{u}$ and v by

$$\boldsymbol{\varphi}(\boldsymbol{x}) = (x_1 + u_1) \boldsymbol{r}^1(x_2) + (\zeta x_2 + u_2) \boldsymbol{r}^2(x_2) + v \boldsymbol{r}^3(x_2),$$

[4] This is not a proof: for that, see [16] [12].

where $\zeta = 1 - \frac{1}{2}\omega^2\xi^2$ measures the amount by which the ribbon is compressed. This also depends on ω: we would like a theory in which part of the ribbon (but not all) is under tension, and therefore almost helicoidal in the lowest-energy state. If the ribbon is only slightly twisted, then naturally it should also be only slightly compressed.

The first derivatives of $\boldsymbol{\varphi}$ are given by

$$\begin{aligned}\partial_1\boldsymbol{\varphi} &= (1+\partial_1 u_1)\boldsymbol{r}^1 + (\partial_1 u_2)\boldsymbol{r}^2 + (\partial_1 v)\boldsymbol{r}^3\\ \partial_2\boldsymbol{\varphi} &= (\partial_2 u_1 - \omega v)\boldsymbol{r}^1 + (\zeta + \partial_2 u_2)\boldsymbol{r}^2 + (\partial_2 v + \omega x_1 + \omega u_1)\boldsymbol{r}^3,\end{aligned}$$

so the induced metric is approximated by

$$\nabla\boldsymbol{\varphi}^T\nabla\boldsymbol{\varphi} = \mathrm{Id} + 2\,\mathrm{e}(\boldsymbol{u}) + \begin{pmatrix}(\partial_1 v)^2 & (\partial_2 v + \omega x_1)\partial_1 v - \omega v\\ \cdots & (\partial_2 v + \omega x_1)^2 - \omega^2\xi^2\end{pmatrix} + O(\omega^4). \tag{6}$$

We turn to the second fundamental form. The normal is given by

$$\boldsymbol{n} = \frac{\partial_1\boldsymbol{\varphi}\times\partial_2\boldsymbol{\varphi}}{|\partial_1\boldsymbol{\varphi}\times\partial_2\boldsymbol{\varphi}|} = O(\omega)\boldsymbol{r}^1 + O(\omega)\boldsymbol{r}^2 + (1+O(\omega^2))\boldsymbol{r}^3,$$

and the second fundamental form $(\mathrm{I\!I}_{\boldsymbol{\varphi}})_{ij} = \boldsymbol{n}\cdot\partial_{ij}\boldsymbol{\varphi}$ is approximately

$$\mathrm{I\!I}_{\boldsymbol{\varphi}} = \nabla\nabla v + \begin{pmatrix}0 & \omega\\ \omega & 0\end{pmatrix} + O(\omega^3). \tag{7}$$

By substituting our approximations of the membrane term (Equation 6) and bending term (Equation 7) into the nonlinear energy (Equation 5) we see that

$$I^{(h)}(\boldsymbol{\varphi}) = \int_\Omega |\mathbf{M}|^2 + h^2|\mathbf{B}|^2\,\mathrm{d}\boldsymbol{x} + O(\omega^6, h^2\omega^4),$$

which is the small-displacement, small-slope energy $E^{(h)}$, plus a small error.

Finally, we note that both Green [19] and Chopin and Kudrolli [11] clamped the top and bottom of the ribbon, then twisted the clamps. In the present setting, this yields boundary data at the top and bottom: $\boldsymbol{u}(x_1,0) = \boldsymbol{u}(x_1,l) = \mathbf{0}$ and $v(x_1,0) = v(x_1,l) = 0$.

It is reasonable, given that the justification of Equation (2) above is far from a proof, to ask why we do not work directly with a nonlinear energy. Indeed, the wrinkling of a thin sheet can be studied from either a fully nonlinear perspective or in a small-slope framework. Both approaches have advantages: a fully nonlinear theory is more physically compelling, but the small-slope setting allows us to describe wrinkling via the same mechanism with simpler arguments. We seek a better understanding of the physical causes of wrinkling, so we choose the simplest setting in which these causes are present.

2.3 The relaxed energy and the identification of $\mathcal{E}_0$

An immediate consequence of Theorem 1 is that $\lim_{h\to 0} \min E^{(h)} = \mathcal{E}_0$. A natural guess is that we should simply set $h = 0$ in the definition of $E^{(h)}$ (Equation 2), and minimize the resulting energy. This is almost correct, but with a wrinkle: the minimum is not achieved. It is true that $\mathcal{E}_0 = \inf E^{(h=0)}$ subject to the boundary conditions of Theorem 1, but it is useful to consider an energy functional which achieves its minimum. This is called the relaxed energy functional, which we denote by $E^{(h)}$.

It is a familiar physical fact that we can stretch a thin elastic sheet by pulling on the ends, but we cannot easily compress the sheet by pushing the ends together: the sheet can avoid large compressive strains by buckling out of plane. This suggests that, in order to approximate the energy in the limit $h \to 0$, we consider an energy functional that penalizes stretching but assigns 0 energy to compression. Thus, we define the *relaxed energy*:

$$E^{(0)} = \int_\Omega \left|(\mathbf{M})_+\right|^2 \mathrm{d}\boldsymbol{x}. \tag{8}$$

By $(\mathbf{M})_+$ we mean the the positive semidefinite part of $\mathbf{M}$. Specifically, if $\mathbf{M}$ has eigenvalues λ_i, then $(\mathbf{M})_+$ has eigenvalues $\max\{0, \lambda_i\}$ corresponding to the same eigenvectors.

It is immediate that $E^{(0)}(\boldsymbol{u}, v) \le E^{(h)}(\boldsymbol{u}, v)$ for any $\boldsymbol{u}$, v and h. This is all that we need; we use the idea of relaxation in a crucial way, but we do not make use of the general theory.[5] We note for the interested reader that the fact that $E^{(0)}$ is indeed the relaxation of $E^{(h=0)}$ follows from the analogous fact for the von Kármán energy functional for an elastic plate ([13] Equation 1.2) and the integral representation of quasiconvexification ([14] page 424).

Proposition 1 (Minimizing $E^{(0)}$) *The relaxed energy $E^{(0)}(\boldsymbol{u}, v)$ achieves its minimum at $\boldsymbol{u} = \mathbf{0}$, $v = 0$, where the minimum is taken over all $\boldsymbol{u}$ and v satisfying the conditions of Theorem 1.*

Proof This fact follows from a short computation. The key idea is to apply Jensen's Inequality to the integral in x_2 alone.

$$\begin{aligned} E^{(0)}(\boldsymbol{u}, v) &\ge \int_\Omega (m_{22}(\boldsymbol{u}, v))_+^2 \,\mathrm{d}\boldsymbol{x} \\ &= l \int_{-1/2}^{1/2} \frac{1}{l} \int_0^l (m_{22}(\boldsymbol{u}, v))_+^2 \,\mathrm{d}x_2 \,\mathrm{d}x_1 \\ &\ge l \int_{-1/2}^{1/2} \left(\frac{1}{l} \int_0^l m_{22}(\boldsymbol{u}, v) \,\mathrm{d}x_2 \right)_+^2 \mathrm{d}x_1 \end{aligned}$$

[5] For a general introduction to the relaxed energy functional see [14], and for theorems on the relaxation for a two-dimensional sheet in three dimensions see [25].

We substitute in $m_{22} = \partial_2 u_2 + \frac{1}{2}(\partial_2 v)^2 + \omega x_1 \partial_2 v + \frac{1}{2}\omega^2\left(x_1^2 - \xi^2\right)$. The $\partial_2 u_2$ and $\partial_2 v$ terms vanishes when integrated due to the boundary conditions.

$$\begin{aligned} E^{(0)}(\boldsymbol{u}, v) &\geq l \int_{-1/2}^{1/2} \left(\frac{1}{l} \int_0^l \frac{1}{2}(\partial_2 v)^2 \,\mathrm{d}x_2 + \frac{1}{2}\omega^2 \left(x_1^2 - \xi^2\right) \right)_+^2 \mathrm{d}x_1 \\ &\geq l \int_{-1/2}^{1/2} \left(\frac{1}{2}\omega^2 \left(x_1^2 - \xi^2\right) \right)_+^2 \mathrm{d}x_1 \\ &\geq E^{(0)}(\mathbf{0}, 0) \end{aligned}$$

Motivated by this result, we define the *minimum energy* $\mathcal{E}_0 = E^{(0)}(\mathbf{0}, 0)$ and the *excess energy*, defined as

$$\epsilon(\boldsymbol{u}, v) = E^{(h)}(\boldsymbol{u}, v) - \mathcal{E}_0. \tag{9}$$

The fact that $E^{(0)} \leq E^{(h)}$ and the above proposition show that $\epsilon \geq 0$. Note that Theorem 1 asserts that we can find a deformation that makes $\epsilon \lesssim h^{4/3}$.

Our next task is to characterize ϵ in a way that is amenable to upper and lower bounds. For instance, we would like to draw conclusions about $\boldsymbol{u}$ and v given that ϵ is small. It is therefore fruitful to write ϵ as a sum, rather than a difference, of positive quantities.

Proposition 2 (An expression for the excess energy) *For any $\boldsymbol{u}$ and v satisfying the boundary data of Theorem 1,*

$$\epsilon = \int_\Omega \left|\mathbf{M}^{(\mathrm{ex})}\right|^2 + h^2 |\mathbf{B}|^2 + \frac{1}{2}\omega^2 (x_1^2 - \xi^2)_+ (\partial_2 v)^2 \,\mathrm{d}\boldsymbol{x} \tag{10}$$

where $\mathbf{M}^{(\mathrm{ex})}$ is interpreted as the excess strain, defined by

$$\mathbf{M}(\boldsymbol{u}, v) = \mathbf{M}^{(\mathrm{ex})}(\boldsymbol{u}, v) + \frac{1}{2}\omega^2 \left(x_1^2 - \xi^2\right)_+ \boldsymbol{e}^{(2)} \otimes \boldsymbol{e}^{(2)}.$$

By 'excess' strain, we mean the additional strain not accounted for in the minimizer of the relaxed energy. The quantity is also given by

$$\mathbf{M}^{(\mathrm{ex})} = \mathrm{e}(\boldsymbol{u}) + \frac{1}{2}\nabla v \otimes \nabla v + \omega \,\mathrm{sym}\left(\nabla(x_1 v) \otimes \boldsymbol{e}^{(2)}\right) + \begin{pmatrix} 0 & -\omega v \\ -\omega v & \frac{1}{2}\omega^2 (x_1^2 - \xi^2)_- \end{pmatrix}. \tag{11}$$

For scalars x we define $(x)_+ = \max\{x, 0\}$ and $(x)_- = \min\{x, 0\}$.

Proof By expanding the membrane term in $E^{(h)}$,

$$\begin{aligned} E^{(h)} &= \int_\Omega \left| \mathbf{M}^{(\mathrm{ex})} + \frac{1}{2}\omega^2 \left(x_1^2 - \xi^2\right)_+ \boldsymbol{e}^{(2)} \otimes \boldsymbol{e}^{(2)} \right|^2 + h^2 |\mathbf{B}|^2 \,\mathrm{d}\boldsymbol{x} \\ &= \int_\Omega \left|\mathbf{M}^{(\mathrm{ex})}\right|^2 + 2\left\langle \mathbf{M}^{(\mathrm{ex})}, \frac{1}{2}\omega^2 \left(x_1^2 - \xi^2\right)_+ \boldsymbol{e}^{(2)} \otimes \boldsymbol{e}^{(2)} \right\rangle \\ &\quad + \frac{1}{4}\omega^4 \left(x_1^2 - \xi^2\right)_+^2 + h^2 |\mathbf{B}|^2 \,\mathrm{d}\boldsymbol{x}. \end{aligned}$$

Let $a = \int_\Omega \left\langle \mathbf{M}^{(\mathrm{ex})}, \frac{1}{2}\omega^2 \left(x_1^2 - \xi^2\right)_+ \boldsymbol{e}^{(2)} \otimes \boldsymbol{e}^{(2)} \right\rangle \mathrm{d}\boldsymbol{x}$. Using the boundary data and the fact that $(x)_+ (x)_- = 0$ for any scalar x, we see that

$$\begin{aligned} a &= \int_\Omega \frac{1}{2}\omega^2 \left(x_1^2 - \xi^2\right)_+ \left(\partial_2 u_2 + \frac{1}{2}\left(\partial_2 v\right)^2 + \omega x_1 \partial_2 v + \frac{1}{2}\omega^2 \left(x_1^2 - \xi^2\right)_-\right) \mathrm{d}\boldsymbol{x} \\ &= \int_\Omega \frac{1}{4}\omega^2 \left(x_1^2 - \xi^2\right)_+ \left(\partial_2 v\right)^2 \mathrm{d}\boldsymbol{x}. \end{aligned}$$

The result follows from the above and our expression for $E^{(h)}$.

We would like to use the minimizer of $E^{(0)}$ to understand the minimizers of $E^{(h)}$, in the limit $h \to 0$. The guiding principle is that, in order to avoid large compressive strains predicted by the relaxed problem, a thin ribbon can introduce extra arc length by buckling away from the relaxed solution. In the present setting, we know that vertical material lines $x_2 = \text{const}$ are compressed if $|x_1| < \xi$, and stretched if $|x_1| > \xi$, and so we expect that vertical lines with $|x_1| < \xi$ should buckle away from the helix. The excess strain, evaluated at the relaxed solution $(\boldsymbol{u}, v) = (\mathbf{0}, 0)$, reflects this fact:

$$\mathbf{M}^{(\mathrm{ex})}(\mathbf{0}, 0) = -\frac{1}{2}\left(\xi^2 - x_1^2\right)_+ \mathbf{e}_2 \otimes \mathbf{e}_2,$$

which we interpret to mean that material lines in the $\mathbf{e}_2$ direction need to wrinkle so as to introduce extra arc length proportional to $-\frac{1}{2}\left(\xi^2 - x_1^2\right)_+$. The 'extra arc length' introduced locally via normal displacement is $\partial_2 u_2 + \frac{1}{2}(\partial_2 v)^2$. Because our boundary data implies that $\partial_2 u_2$ is mean 0, we draw conclusions about the mean value of $\frac{1}{2}(\partial_2 v)^2$.

Lemma 1 (Wasting the correct amount of arc length) *Let $\epsilon > 0$ be defined via Equation (9), and let $(\boldsymbol{u}, v)$ satisfy the conditions of Theorem 1. The excess energy $\epsilon(\boldsymbol{u}, v)$ satisfies*

$$\int_{-\frac{1}{2}}^{\frac{1}{2}} \left(\int_0^l \frac{1}{2}\left(\partial_2 v\right)^2 - \frac{\omega^2}{2}\left(\xi^2 - x_1^2\right)_+ \mathrm{d}x_2 \right)^2 \mathrm{d}x_1 \leq \epsilon l. \tag{12}$$

Proof From Equation (10), we see that $\int_\Omega \left(m_{22}^{(\mathrm{ex})}\right)^2 \mathrm{d}\boldsymbol{x} \leq \epsilon$. The result follows immediately from Jensen's Inequality and the boundary conditions of Theorem 1: $\int_0^l \partial_2 u_2 \, \mathrm{d}x_2 = \int_0^l \partial_2 v \, \mathrm{d}x_2 = 0$.

Experimentally, we see that the ribbon wrinkles in a certain parameter regime. This is consistent with our discussion, but not an easy consequence of it: there are many deformations that introduce extra arc length, some of which 'wrinkle' in that they oscillate with a small length scale.

3 The lower bound

This section proves the lower bound found in Theorem 1. This proof has two parts. Firstly, in Proposition 3 we show that the outside of the ribbon $\{|x_1| > \xi\}$

is stretched, which should imply that the excess energy ϵ controls the size of the displacements $\boldsymbol{u}$, v in that region. To explain the idea, we first outline a simple but unsuccesful attempt. Intuitively, if the displacement $(\boldsymbol{u}(\boldsymbol{x}), v(\boldsymbol{x}))$ at some point $x_1 > \xi$ is non-zero, then the vertical line connecting the top and the bottom of the sheet must be stretched. As we will see in the proof of Proposition 3, it is straightforward to show that $\partial_2 v$ must be small in L^2 (meaning that, on average, the point cannot be greatly displaced in the normal direction). The idea that *vertical* lines are stretched if the displacements are large suggests that we consider the 22 component of the membrane term. This intuition is partially correct: it shows that $\partial_2 u_2$ must be small (meaning that the point cannot be displaced much in the vertical direction). The major difficulty lies in showing that the point cannot be displaced horizontally, either: u_1 must also be small.

Instead, we consider two *diagonal* lines connecting the top and the bottom of the sheet, and that are contained entirely in the zone $\{|x_1| > \xi\}$ under vertical tension. Let $\boldsymbol{a}^+$ and $\boldsymbol{a}^-$ be the tangent vectors for these diagonal lines. The above argument, using the tension in each of our diagonal directions, gives control on $\boldsymbol{u} \cdot \boldsymbol{a}^+$ and $\boldsymbol{u} \cdot \boldsymbol{a}^-$. This is sufficient to control $\boldsymbol{u}$.[6]

The conclusion of the proof, Proposition 4, is more standard. In the inner region $\{|x_1| < \xi\}$ the relaxed problem predicts some known, $O(1)$ compression; so by Lemma 1 we must waste some known amount of arc length: $\int_0^l (\partial_2 v(x_1, x_2))^2 \, \mathrm{d}x_2$ is a known function of x_1, up to a small error. Since the displacements near the edges of the ribbon are small, the membrane term prefers that the amplitude v of the wrinkles be small, because otherwise horizontal lines across the wrinkles would be stretched. Conversely, the bending energy penalizes small, rapid wrinkles. The competition between membrane and bending energy sets the scale of the minimum energy.

Finally, we remark that this argument makes repeated use of the idea that stretching lines in the ribbon should cost energy. Of course, we are not in a position to say much about *every* material line. The above arguments, more carefully stated, start with the assumption that the membrane tensor $\mathbf{M}$ is small in an L^p sense, meaning that material lines are not stretched much on average.

Proposition 3 (Rigidity of the outer edges) *Let $\boldsymbol{u}$ and v be as in Theorem 1, and let $\epsilon = E^{(h)}(\boldsymbol{u}, v) - \mathcal{E}_0$. There exists some $\xi'_{\text{left}} \in \left(-\frac{1}{2}, -\xi\right)$ and $\xi'_{\text{right}} \in \left(\xi, \frac{1}{2}\right)$,*

$$\|v(\xi', \cdot)\|_{L^\infty} \lesssim \epsilon^{1/2}, \text{ and} \tag{13}$$

$$\left| \int_0^l u_1(\xi', x_2) \, \mathrm{d}x_2 \right| \lesssim \epsilon^{1/2}, \tag{14}$$

for both $\xi' = \xi'_{\text{left}}$ and $\xi' = \xi'_{\text{right}}$.

We remind the reader of the distinction between $\lessapprox$ and $\lesssim$ (Remark 1). On first reading, we suggest treating ξ and l as constants, keeping only the dependence on h and ϵ.

Proof Let $\xi_0 = \frac{1}{2}\left(\xi + \frac{1}{2}\right)$.

[6] This argument is due to M. Strauss [26], who used it to show that control on $\mathrm{e}(\boldsymbol{u})$ in L^1 yields control on $\boldsymbol{u}$.

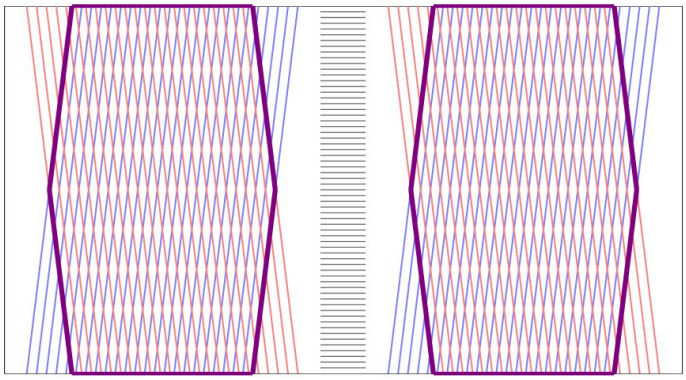

Fig. 3: A sketch of $\Omega^{\pm}$.
Ω^{+}: regions filled with positively sloped diagonal lines (blue online).
Ω^{-}: regions filled with negatively sloped diagonal lines (red online).
Ω^{0}: Two hexagons $\Omega^{+} \cap \Omega^{-}$. Outlined with thick lines (purple online).

From Equation (10) we see that $\epsilon \geq \frac{1}{2}\omega^2(\xi_0^2 - \xi^2) \int_{\{|x_1|>\xi_0\}} (\partial_2 v)^2 \, \mathrm{d}\boldsymbol{x}$, so

$$\|\partial_2 v\|_{L^2(\{|x_1|>\xi_0\})} \leq \frac{2^{1/2}\epsilon^{1/2}}{\omega\left(\xi_0^2 - \xi^2\right)^{1/2}} \lessapprox \frac{\epsilon^{1/2}}{\left(\frac{1}{2} - \xi\right)^{1/2}}. \tag{15}$$

We are now able to prove Equation (13), but because we must find some ξ'_{left} and ξ'_{right} that work for both parts of the proposition we will hold off.

Step 1: control of ∇v. We proceed with the 'diagonal lines' argument outlined at the beginning of this section. Let $\alpha = \frac{1}{5l}\left(\frac{1}{2} - \xi_0\right)$, and let $\boldsymbol{a}^{\pm}$ be a unit vector in the direction $(\pm\alpha, 1)$.[7] We define the sets Ω^{+}, Ω^{-} and $\Omega^{0} = \Omega^{+} \cap \Omega^{-}$ as shown in Figure 3. Specifically, $\Omega^{\pm}$ are the maximal open sets with the following properties:

- $\Omega^{\pm}$ is the union of two parallelograms in Ω, one of which satisfies $x_1 \in \left(-\frac{1}{2}, \xi\right)$ and the other $x_1 \in \left(\xi, \frac{1}{2}\right)$, and
- two sides (of each parallelogram) are parallel to $\boldsymbol{a}^{\pm}$, and
- the other two sides are contained in the top $\{x_2 = l\}$ and bottom $\{x_2 = 0\}$ of the ribbon.

The key geometric properties of these definitions follow.

1. Consider some point $\boldsymbol{x}$ with $\xi_0 < |x_1| < \frac{1}{2}$. This point is in $\Omega^{\pm}$ if and only if the line segment passing through $\boldsymbol{x}$, parallel to $\boldsymbol{a}^{\pm}$ and connecting the top of the ribbon ($x_2 = l$) with the bottom ($x_2 = 0$) is contained entirely in the outer region $\{|x_1| > \xi_0\}$.
2. The slope α^{-1} is large enough that intersection Ω^{0} contains a rectangle connecting the top of the domain to the bottom.

[7] In the sequel we will make many statements that hold for both $\boldsymbol{a}^{+}$ and $\boldsymbol{a}^{-}$. Any statement containing $\pm$ should be interpreted as *two* statements, one with $\pm$ everywhere replaced with $+$, and a similar one with $-$.

We are now ready to prove Equation (13). In fact we will choose ξ'_{left} and ξ'_{right} near the center of the hexagons Ω^0, which will help in the proof of Equation (14). Let $\xi_1 = \xi_0 + 2\alpha l$ and $\xi_2 = \frac{1}{2} - 2\alpha l$. Recalling our control on $\partial_2 v$ (Equation 15), we have that

$$\begin{aligned}\int_{\xi_1}^{\xi_2} \|v(x_1,\cdot)\|^2_{L^\infty(0,l)}\,\mathrm{d}x_1 &\le l\|\partial_2 v\|^2_{L^2((\xi_1,\xi_2)\times(0,l))}\\ &\le \frac{2\epsilon l}{\omega^2\left(\xi_0^2-\xi^2\right)} \lessapprox \frac{\epsilon l}{\frac{1}{2}-\xi_0} \lesssim \epsilon.\end{aligned}$$

We conclude that there exists some $\xi'_{\text{right}} \in (\xi_1, \xi_2)$ such that

$$\|v(\xi'_{\text{right}},\cdot)\|_{L^\infty} \lessapprox \frac{\epsilon^{1/2} l^{1/2}}{\frac{1}{2}-\xi} \lesssim \epsilon^{1/2}. \tag{16}$$

Similarly, there is some $\xi'_{\text{left}} \in (-\xi_2, -\xi_1)$ such that $v(\xi'_{\text{left}},\cdot)$ satisfies the same bounds.

Using Equation (10), we see that

$$\epsilon \ge \int_{\Omega^\pm} \left\langle \boldsymbol{a}^\pm, \mathbf{M}^{(\text{ex})}\boldsymbol{a}^\pm\right\rangle^2 \mathrm{d}\boldsymbol{x}$$

so by Jensen's Inequality

$$\begin{aligned}\left|\Omega^\pm\right|^{1/2}\epsilon^{1/2} &\ge \int_{\Omega^\pm}\left\langle \boldsymbol{a}^\pm, \mathbf{M}^{(\text{ex})}\boldsymbol{a}^\pm\right\rangle \mathrm{d}\boldsymbol{x}\\ &\ge \int_{\Omega^\pm} \partial_\pm(\boldsymbol{u}\cdot\boldsymbol{a}^\pm) + (\boldsymbol{a}^\pm\cdot\boldsymbol{e}^{(2)})\omega\partial_\pm(x_1 v)\\ &\qquad - \frac{\pm 2\alpha}{1+\alpha^2}\omega v + \frac{1}{2}\left(\boldsymbol{a}^\pm\cdot\nabla v\right)^2 \mathrm{d}\boldsymbol{x}\end{aligned}$$

where $\partial_\pm = \boldsymbol{a}^\pm\cdot\nabla$ is the directional derivative in the direction of $\boldsymbol{a}^\pm$. By the boundary conditions, the first two terms integrate to 0 and so we get that

$$\begin{aligned}\int_{\Omega^\pm}\frac{1}{2}\left(\boldsymbol{a}^\pm\cdot\nabla v\right)^2 &\le \left|\Omega^\pm\right|^{1/2}\epsilon^{1/2} + 2\alpha\omega\,\|v\|_{L^1\{|x_1|>\xi_0\}}\\ &\lessapprox \left|\Omega^\pm\right|^{1/2}\epsilon^{1/2} + \alpha\left(\frac{1}{2}-\xi\right)^{1/2} l^{3/2}\,\|\partial_2 v\|_{L^2\{|x_1|>\xi_0\}}\end{aligned}$$

The control on v (Equation 15) implies that

$$\int_{\Omega^\pm}\left(\boldsymbol{a}^\pm\cdot\nabla v\right)^2 \lessapprox \left|\Omega^\pm\right|^{1/2}\epsilon^{1/2} + \alpha l^{3/2}\epsilon^{1/2} \lesssim \epsilon^{1/2}. \tag{17}$$

We recall that $\alpha \lessapprox \frac{\frac{1}{2}-\xi}{l}$, so both terms are controlled by

$$\int_{\Omega^\pm}\left(\boldsymbol{a}^\pm\cdot\nabla v\right)^2 \lessapprox l^{1/2}\left(\frac{1}{2}-\xi\right)^{1/2}\epsilon^{1/2} \lesssim \epsilon^{1/2}.$$

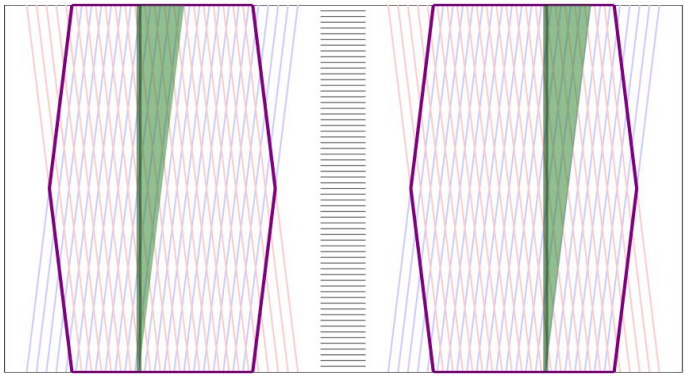

Fig. 4: A sketch of the domain $\blacktriangle^+$.
$\Omega^\pm$, Ω^0: carried over from Figure 3.
$x_1 = \xi'_{\text{left}}$ or ξ'_{right}: thick vertical lines (dark green online).
$\blacktriangle^+$: triangular shaded regions (light green online).

Step 2: a trace-like inequality on $\boldsymbol{u}$. We invoke a similar diagonal lines argument to control $\boldsymbol{u}$ along vertical lines and so prove Equation (14). [8] Specifically, we control

$$\int_0^l u_1(\xi', x_2)\,\mathrm{d}x_2 = \int_0^l \frac{\sqrt{1+\alpha^2}}{2\alpha}\left(\boldsymbol{a}^+ - \boldsymbol{a}^-\right)\cdot\boldsymbol{u}(\xi', x_2)\,\mathrm{d}x_2$$

by controlling $\int \boldsymbol{a}^+\cdot\boldsymbol{u}(\xi', x_2)\,\mathrm{d}x_2$ and $\int \boldsymbol{a}^-\cdot\boldsymbol{u}(\xi', x_2)\,\mathrm{d}x_2$ separately.

We note that $\boldsymbol{u}$, pointwise, can be expressed by integrating along lines:

$$\begin{aligned}\boldsymbol{a}^\pm\cdot\boldsymbol{u}(\xi', x_2) &= \int_0^{x_2(1+\alpha^2)^{1/2}} \partial_\pm\left(\boldsymbol{a}^\pm\cdot\boldsymbol{u}(\boldsymbol{x}+s\boldsymbol{a}^\pm)\right)\mathrm{d}s\\ &= \int_0^{x_2(1+\alpha^2)^{1/2}} \left\langle \boldsymbol{a}^\pm, \mathrm{e}(\boldsymbol{u})(\boldsymbol{x}+s\boldsymbol{a}^\pm)\boldsymbol{a}^\pm\right\rangle \mathrm{d}s.\end{aligned}$$

Integrating over x_2 and using a change of variables, we see that traces of $\boldsymbol{u}$ are determined by $\mathrm{e}(\boldsymbol{u})$:

$$\int_0^l \boldsymbol{a}^\pm\cdot\boldsymbol{u}(\xi', x_2)\,\mathrm{d}x_2 = \frac{\sqrt{1+\alpha^2}}{\alpha}\int_{\blacktriangle^\pm}\left\langle \boldsymbol{a}^\pm, \mathrm{e}(\boldsymbol{u})\boldsymbol{a}^\pm\right\rangle \mathrm{d}\boldsymbol{x}. \tag{18}$$

The domain of integration $\blacktriangle^\pm$ is a right triangle contained in the right half of Ω^0, as shown in Figure 4. One side is $\{\xi'\}\times(0,l)$, and the hypotenuse is parallel to $\boldsymbol{a}^\pm$. In particular, note that $\blacktriangle^\pm \subseteq \Omega^0$.

By Equation (11), we express $\mathrm{e}(\boldsymbol{u})$ in the following form:

$$\mathrm{e}(\boldsymbol{u}) = \mathbf{M}^{(\mathrm{ex})} - \frac{1}{2}\nabla v\otimes\nabla v - \omega\,\mathrm{sym}\left(\nabla(x_1 v)\otimes\boldsymbol{e}^{(2)}\right) + v\begin{pmatrix}0 & \omega\\ \omega & 0\end{pmatrix} \tag{19}$$

[8] This argument is closely connected to the trace inequality in BD. We have L^1 control on $\mathrm{e}(\boldsymbol{u})$ and would like control on the trace of $\boldsymbol{u}$. This does not follow directly from Korn's Inequality (which requires L^p control, for $p>1$), but it follows from the trace inequality in BD [28] [3]. Because we would like to know how the constant depends on ξ and l we prove the result directly.

Our goal is to bound $\int_{\blacktriangle^\pm} \left\langle \boldsymbol{a}^\pm, \mathrm{e}(\boldsymbol{u})\boldsymbol{a}^\pm \right\rangle \mathrm{d}\boldsymbol{x}$ by controlling these four quantities. From Equation (10) we see immediately that

$$\alpha^{-1} \int_{\blacktriangle^\pm} \left\langle \boldsymbol{a}^\pm, \mathbf{M}^{(\mathrm{ex})} \boldsymbol{a}^\pm \right\rangle \mathrm{d}\boldsymbol{x} \lessapprox \alpha^{-1} \epsilon^{1/2} \left| \blacktriangle^\pm \right|^{1/2} \lessapprox l^{3/2} \left(\frac{1}{2} - \xi_0 \right)^{-1/2} \epsilon^{1/2}$$

Equation (17) controls ∇v, so

$$\alpha^{-1} \int_{\blacktriangle^\pm} \left\langle \boldsymbol{a}^\pm, [\nabla v \otimes \nabla v]\, \boldsymbol{a}^\pm \right\rangle \mathrm{d}\boldsymbol{x} \lessapprox l^{3/2} \left(\frac{1}{2} - \xi_0 \right)^{-1/2} \epsilon^{1/2}.$$

The next term is, pointwise, too large in ϵ for our purposes. We invoke the fundamental theorem of calculus:

$$\begin{aligned} \alpha^{-1} \int_{\blacktriangle^\pm} \left\langle \boldsymbol{a}^\pm, \mathrm{sym}\left(\nabla(x_1 v) \otimes \boldsymbol{e}^{(2)} \right) \boldsymbol{a}^\pm \right\rangle \mathrm{d}\boldsymbol{x} &= \frac{\alpha^{-1}}{\sqrt{1+\alpha^2}} \int_{\blacktriangle^\pm} \left\langle \boldsymbol{a}^\pm, \nabla(x_1 v) \right\rangle \mathrm{d}\boldsymbol{x} \\ &= \frac{|\xi'|}{1+\alpha^2} \int_0^l v(\xi', x_2)\, \mathrm{d}x_2 \lesssim \epsilon^{1/2}. \end{aligned}$$

Finally, we bound the last term in Equation (19).

$$\begin{aligned} \alpha^{-1} \int_{\blacktriangle^\pm} \left| \left\langle \boldsymbol{a}^\pm, \begin{pmatrix} 0 & \omega v \\ \omega v & 0 \end{pmatrix} \boldsymbol{a}^\pm \right\rangle \right| \mathrm{d}\boldsymbol{x} &= \frac{\pm\omega}{1+\alpha^2} \int_{\blacktriangle^\pm} |v(\boldsymbol{x})| \\ &\lessapprox l \int_{\xi_1}^{\xi_2} \|v(x_1, \cdot)\|_{L^\infty}\, \mathrm{d}x_1 \\ &\le l(\xi_2 - \xi_1)^{1/2} \sqrt{\int_{\xi_1}^{\xi_2} \|v(x_1, \cdot)\|_{L^\infty}^2\, \mathrm{d}x_1} \\ &\lessapprox l^{3/2} \epsilon^{1/2}. \end{aligned}$$

Equation (14) follows from the bounds of the above paragraph, Equation (18), and the fact that $u_1 = \frac{\sqrt{1+\alpha^2}}{2\alpha} \left(\boldsymbol{a}^+ - \boldsymbol{a}^- \right) \cdot \boldsymbol{u}$. Specifically, we have shown that

$$\left| \int_0^l u_1(\xi', x_2)\, \mathrm{d}x_2 \right| \lessapprox \epsilon^{1/2} l^{5/2} \left(\xi_0 - \xi \right)^{-3/2}. \tag{20}$$

We are in position to complete the proof of the lower bound in Theorem 1, but first we summarize the argument. This is similar to the lower bound in [5].

We now know that the displacements are small outside the wrinkled zone. But we have also assumed that the energy is small, which in particular implies that *horizontal* lines connecting ξ'_{left} and ξ'_{right} cannot be stretched much. Combining these facts, we see that the amplitude of the wrinkles must be small (in L^2, not pointwise).

Proposition 4 (The lower bound) *There is some constant C such that, for any $\boldsymbol{u}$ and v satisfying the boundary conditions of Theorem 1,*

$$E^{(h)}(\boldsymbol{u}, v) \ge \mathcal{E}_0 + C h^{4/3}.$$

The constant C depends on ω, ξ and l but not h.

Proof By considering the bending term in Equation (2), we see immediately that

$$\int_\Omega (\partial_{22} v)^2 \,\mathrm{d}\boldsymbol{x} \leq h^{-2}\epsilon. \tag{21}$$

In fact, it will be useful to consider a smaller domain $\Omega' = \left\{\xi'_{\text{left}} < x_1 < \xi'_{\text{right}}\right\}$ in which we have better control.

We establish control on $\int_{\Omega'} v^2 \,\mathrm{d}\boldsymbol{x}$ by controlling $\partial_1 v$. By examining the 11 component of the membrane term in Equation (2), we have that

$$\begin{aligned}\epsilon &\geq \int_{\Omega'} m_{11}^2 \,\mathrm{d}\boldsymbol{x} \gtrapprox \frac{1}{l}\left(\int_{\Omega'} m_{11}\,\mathrm{d}\boldsymbol{x}\right)^2 \\ &\geq \frac{1}{l}\left(\frac{1}{2}\int_{\Omega'}(\partial_1 v)^2\,\mathrm{d}\boldsymbol{x} - \left|\int_{\Omega'}\partial_1 u_1\,\mathrm{d}\boldsymbol{x}\right|\right)^2\end{aligned}$$

We use this to bound $\int_{\Omega'}(\partial_1 v)^2\,\mathrm{d}\boldsymbol{x}$ in terms of u_1 and ϵ, then invoke Equation (20).

$$\begin{aligned}\int_{\Omega'}(\partial_1 v)^2\,\mathrm{d}\boldsymbol{x} &\lessapprox \epsilon^{1/2} l^{1/2} + \left|\int_0^l u_1(\xi'_{\text{right}}, x_2) - u_1(\xi'_{\text{left}}, x_2)\,\mathrm{d}x_2\right| \\ &\lessapprox \epsilon^{1/2} l^{5/2}\left(\xi_0 - \xi\right)^{-3/2}.\end{aligned}$$

The Sobolev embedding inequality, together with the control of v on $\{x_1 = \xi'\}$ (Equation 16), yields that

$$\int_{\Omega'} v^2\,\mathrm{d}\boldsymbol{x} \lessapprox \epsilon^{1/2} l^{5/2}\left(\frac{1}{2}-\xi\right)^{-3/2} + \epsilon l^2\left(\frac{1}{2}-\xi\right)^{-2} \tag{22}$$

We are now ready to use a simple interpolation inequality to bound the slopes from above.

$$\int_{\Omega'}(\partial_2 v)^2\,\mathrm{d}\boldsymbol{x} \leq \left(\int_{\Omega'} v^2\,\mathrm{d}\boldsymbol{x}\right)^{1/2}\left(\int_{\Omega'}(\partial_{22}v)^2\,\mathrm{d}\boldsymbol{x}\right)^{1/2} \lesssim \epsilon^{3/4}h^{-1} \tag{23}$$

On the other hand, we know (by Lemma 1) that the wrinkles must relax a fixed amount of contraction, so the slopes are bounded from above in L^2. By Equation (12) and Jensen's Inequality,

$$\left|\int_{\Omega'}\frac{1}{2}(\partial_2 v)^2 - \frac{\omega^2}{2}\left(\xi^2 - x_1^2\right)_+\right|\mathrm{d}\boldsymbol{x} \leq \epsilon^{1/2} l^{1/2},$$

so therefore

$$\int_{\Omega'}\frac{1}{2}(\partial_2 v)^2\,\mathrm{d}\boldsymbol{x} \geq \int_{\{|x_1|<\xi\}}\frac{1}{2}\left(\xi^2 - x_1^2\right)^2\mathrm{d}\boldsymbol{x} - \epsilon^{1/2}l^{1/2} \gtrsim 1. \tag{24}$$

Equation (23) and the above equation show that $\epsilon^{3/4}h^{-1} \gtrsim 1$, which proves the lower bound.

Proposition 5 (Lower bound with multiple parameters) *Let $\boldsymbol{u}$ and v satisfy the conditions of Theorem 1. For h sufficiently small, $l \geq 1$ and $\xi \in (0, 1/4)$,*

$$\epsilon \gtrapprox h^{4/3} l^{-1/3}\left(\frac{1}{2}-\xi\right). \tag{25}$$

Proof Using Equation (21) and (22), we get that

$$\int_{\Omega'} (\partial_2 v)^2 \, \mathrm{d}\boldsymbol{x} \lessapprox \epsilon^{3/4} l^{5/4} \left(\frac{1}{2} - \xi\right)^{3/4} h^{-1} + \epsilon l^{-1} \left(\frac{1}{2} - \xi\right)^{-1} h^{-1}.$$

Combining this with Equation (24) yields

$$\epsilon^{3/4} l^{5/4} \left(\frac{1}{2} - \xi\right)^{-3/4} h^{-1} + \epsilon l^{1} \left(\frac{1}{2} - \xi\right)^{-1} h^{-1} \gtrapprox l - \epsilon^{1/2} l^{1/2},$$

so

$$\epsilon \gtrapprox \min\left\{ h^{4/3} l^{-1/3} \left(\frac{1}{2} - \xi\right), h \left(\frac{1}{2} - \xi\right), l^{1/2} \right\}.$$

Given the conditions that $l \geq 1$, h is sufficiently small and $\xi \in (0, 1/4)$ the first argument of the minimum is always the smallest. Equation (25) follows.

4 The upper bound

We complete the proof of Theorem 1 by constructing a deformation that achieves $E^{(h)}(\boldsymbol{u}, v) \leq \mathcal{E}_0 + C' h^{4/3}$.

The present task, in short, is to find an 'almost optimal' deformation $(\boldsymbol{u}, v)$. In proving the lower bound we understood something about how any such deformation must behave.

- The normal displacement v must be small for $|x_1| > \xi$ (at least on average), as shown in Equation (15).
- For $|x_1| < \xi$, material lines in the x_2 direction must avoid compression by deviating from the helix. Equation (12) makes this quantitative: $\int_0^l (\partial_2 v)^2 \, \mathrm{d}x_2 = l\omega^2 \left(\xi^2 - x_1^2\right)_+ + o(1)$.
- The amplitude of the wrinkles is small (Equation 22): $\|v\|_{L^2(|x_1|<\xi)} \lesssim h^{1/3}$.

The last two conditions suggest that we should consider a displacement v which oscillates rapidly (with wavelength no more than order $h^{1/3}$). This is our first hint that the minimizer of $E^{(h)}$ is aptly described as 'wrinkling'.

In Example 1 we present an ansatz which, although natural, fails to achieve the correct energy scaling. However, Example 1 is a simple and concrete setting which contains ideas used in the successful argument, and the manner in which our simple ansatz fails motivates the argument that succeeds. The impatient reader can skip directly to Section 4.1; the argument given there is self-contained.

Example 1 (Wrinkling with uniform wavelength: an unsuccessful ansatz) With the above conditions in mind, it is natural to consider a deformation that wrinkles in the x_2 direction with a single wavelength, but with amplitude that varies with x_1. Thus we consider

$$v^{(h)}(\boldsymbol{x}) = \lambda f(x_1) \sin\left(\frac{x_2}{\lambda}\right), \tag{26}$$

where the wavelength is $\lambda = h^{1/3}$ and the amplitude λf is given by

$$f(x_1) = \omega \sqrt{2 \left(\xi^2 - x_1^2\right)_+}. \tag{27}$$

The difficulty is that v is not sufficiently regular, and so we get *infinite* energy.

Step 1: calculating the bending energy. We have yet to define the normal displacement $\boldsymbol{u}^{(h)}$, but recall that the bending energy $\mathbf{B}(v^{(h)}) = \nabla\nabla v^{(h)} + \omega\,(\mathbf{e}_1 \otimes \mathbf{e}_2 + \mathbf{e}_2 \otimes \mathbf{e}_1)$ depends on $v^{(h)}$ alone. We calculate:

$$\begin{aligned} E^{(h)}(\boldsymbol{u}, v^{(h)}) &\geq h^2 \int_\Omega \left|\mathbf{B}(v^{(h)})\right|^2 \mathrm{d}\boldsymbol{x} \\ &= h^2 \int_\Omega \left(\partial_{11} v^{(h)}\right)^2 + \left(\partial_{12} v^{(h)} + \omega\right)^2 + \left(\partial_{22} v^{(h)}\right)^2 \mathrm{d}\boldsymbol{x} \\ &\gtrsim h^2 \int_\Omega h^{2/3} \left(\partial_{11} f(\boldsymbol{x})\right)^2 + \left(\partial_1 f(\boldsymbol{x})\right)^2 + h^{-2/3} \left(f(\boldsymbol{x})\right)^2 \mathrm{d}\boldsymbol{x} \\ &\gtrsim \int_0^\xi h^{8/3} r^{-3} + h^2 r^{-1} + h^{4/3} r \,\mathrm{d}r = \infty. \end{aligned}$$

The last line used that $\partial_1^j f(\boldsymbol{x})$ blows up like $|\xi - x_1|^{1/2-j}$ for x_1 near ξ.

We expect an energy scaling of the form $\min E^{(h)} = \mathcal{E}_0 + O(h^{4/3})$ (Theorem 1). The argument above shows us that the energy of this ansatz is infinite, but the infinite term is formally much smaller than $h^{4/3}$. This gives us the hope that smoothing f slightly could yield the correct energy scaling. However, we will show that the membrane energy is not as well behaved: formally, the coefficient next to the $h^{4/3}$ term is infinite.

Step 2a: vertical stretching. The membrane term controlling stretching in the vertical direction is $m_{22} = \partial_2 u_2^{(h)} + \frac{1}{2}(\partial_2 v^{(h)} + \omega x_1)^2 - \frac{1}{2}\omega^2\xi^2$. Outside the wrinkled zone, the ribbon is purely in tension, which gives us the leading-order energy $\int_{|x_1|>\xi} m_{22}^2 \,\mathrm{d}\boldsymbol{x} = \mathcal{E}_0$. Inside the wrinkled zone, we write this as

$$\begin{aligned} m_{22}(\boldsymbol{x}) &= \partial_2 u_2^{(h)}(\boldsymbol{x}) + \frac{1}{2}\left(f(x_1)\cos\left(\frac{x_2}{\lambda}\right) + \omega x_1\right)^2 - \frac{\omega^2}{2}\xi^2 \\ &= \partial_2 u_2^{(h)}(\boldsymbol{x}) + \frac{1}{4} f^2(x_1)\cos\left(\frac{2x_2}{\lambda}\right) + \omega x_1 f(x_1)\cos\left(\frac{x_2}{\lambda}\right) \\ &:= \partial_2 u_2^{(h)}(\boldsymbol{x}) + \vartheta^{(h)}(\boldsymbol{x}) + \omega x_1 f(x_1)\cos\left(\frac{x_2}{\lambda}\right), \end{aligned}$$

where the remainder $\vartheta^{(h)}$ is $O(1)$. In order to achieve small energy we pick $\partial_2 u_2^{(h)} = -\vartheta^{(h)} - \omega x_1 \partial_2 v^{(h)}$. Note that we must have $u_2^{(h)}(x_1, 0) = u_2^{(h)}(x_1, l) = 0$, which is possible because the remainder integrates to 0 in x_2.[9]

Step 2b: shear energy. Except where we explicitly say otherwise, for the rest of this example we consider only $|x_1| < \xi$.[10] The shear component of the membrane

[9] Our only concrete requirement on $v^{(h)}$ is that it must 'waste the correct amount of arc length' Lemma 1. That $\vartheta^{(h)}$ integrates to 0 in x_2 is equivalent to asserting that the left hand side of Equation (12) is 0, rather than being merely small.

[10] $\boldsymbol{u}^{(h)}(\boldsymbol{x}) = \mathbf{0}$ for $|x_1| > \xi$.

energy is given by

$$\begin{aligned} 2m_{12} &= \partial_2 u_1^{(h)} + \partial_1 u_2^{(h)} + (\partial_2 v^{(h)} + \omega x_1)\partial_1 v^{(h)} - \omega v^{(h)} \\ &= \partial_2 u_1^{(h)} + \frac{1}{2}\lambda\omega^2 x_1 \sin\left(\frac{2x_2}{\lambda}\right) - \lambda\omega(x_1 f(x_1))' \sin\left(\frac{x_2}{\lambda}\right) \\ &\quad + (\partial_2 v^{(h)} + \omega x_1)\partial_1 v^{(h)} - \omega v^{(h)} \\ &= \partial_2 u_1^{(h)} - \lambda\left(\frac{\omega^2}{2} x_1 \sin\left(\frac{2x_2}{\lambda}\right) + 2\omega f(x_1)\sin\left(\frac{x_2}{\lambda}\right)\right). \end{aligned}$$

We aim to achieve $\int |\mathbf{M}|^2 \,\mathrm{d}\boldsymbol{x} \lesssim h^{4/3}$, so this is not small enough. Therefore we choose $\partial_2 u_1^{(h)}$ such that $m_{12} = 0$, noting that the boundary data $u_1^{(h)}(x_1, 0) = u_1^{(h)}(x_1, l) = 0$ is compatible with this because the proposed $\partial_2 u_1^{(h)}$ integrates to 0 in x_2.

We pause to highlight an important idea. We picked $\partial_2 u_2^{(h)}$ to make $m_{22} = 0$. This introduced a non-zero term in m_{12}, which we obtained by differentiating $\vartheta^{(h)}$ in x_1 and integrating it in x_2. Because $\vartheta^{(h)}$ oscillates with wavelength $\lambda = h^{1/3}$ in x_2, $\partial_1 u_2^{(h)}$ is formally smaller but less regular than $\partial_2 u_2^{(h)}$. We are free to play this game again and choose $\partial_2 u_1^{(h)}$ to make $m_{12} = 0$, at the cost of a non-zero term $\partial_1 u_1^{(h)}$ in m_{11}. Again, $\partial_1 u_1^{(h)}$ is smaller but less regular than $\partial_2 u_1^{(h)}$. The loss of regularity is fatal: $\partial_2 u_1^{(h)}$ has a term of the form $x_1 \sin\left(\frac{2x_2}{\lambda}\right) \mathbb{1}_{|x_1|<\xi}$, which is not differentiable. We persist regardless; in fact, we will see that our choice of $v^{(h)}$ always gives infinite membrane energy.

Step 2c: horizontal stretching. The final component in the membrane tensor is

$$\begin{aligned} m_{11} &= \partial_1 u_1^{(h)} + \frac{1}{2}\left(\partial_1 v^{(h)}\right)^2 \\ &= -\lambda^2\left(\frac{\omega^2}{4}\cos\left(\frac{2x_2}{\lambda}\right) + 2\omega f'(x_1)\cos\left(\frac{x_2}{\lambda}\right)\right) + \frac{1}{2}\lambda^2\left(f'(\boldsymbol{x})\right)^2 \sin^2\left(\frac{x_2}{\lambda}\right) \\ &= -\lambda^2\left(\frac{\omega^2 + \left(f'(x_1)\right)^2}{4}\cos\left(\frac{2x_2}{\lambda}\right) + 2\omega f'(x_1)\cos\left(\frac{x_2}{\lambda}\right)\right) + \frac{1}{4}\lambda^2\left(f'(\boldsymbol{x})\right)^2. \end{aligned}$$

This component of $\mathbf{M}$ scales as $h^{2/3}$, meaning that $\int_\Omega |\mathbf{M}|^2 \,\mathrm{d}\boldsymbol{x}$ formally scales as $h^{4/3}$. However, the above expression for m_{11} is *not* in L^2, and so it integrates to infinity. Unlike the bending energy, the infinite term in the membrane energy is formally of leading order. The fatal flaw lies firmly with our choice of $v^{(h)}$: by invoking Parseval's Theorem in the $\mathrm{d}x_2$ integral and disgarding all but the wavenumber 0 term, we see that

$$\begin{aligned} \int_\Omega |m_{11}|^2 \,\mathrm{d}\boldsymbol{x} &= \int_\Omega \left(\partial_1 u_1^{(h)} + \frac{1}{2}(\partial_1 v^{(h)})^2\right)^2 \mathrm{d}\boldsymbol{x} \\ &\gtrsim \int_{-\xi}^{\xi} \lambda^4 (f'(x_1))^4 \,\mathrm{d}x_1 = \infty. \end{aligned}$$

This last estimate, together with step 2a, suggests that we cannot salvage this ansatz by smoothing f in a boundary layer. If the boundary layer is small in h then

the above integral is large in h, but if the boundary layer is not small in h then the vertical stretching term contributes $O(1)$ energy. Our method for choosing $\boldsymbol{u}^{(h)}$ from $v^{(h)}$ is sound, but we must consider a richer class of normal displacements $v^{(h)}$.

The ansatz Equation (26) uses *the same* frequency everywhere in the wrinkled zone, and then varies the amplitude with x_1 to waste the correct amount of arc length (Equation 12). The essential difficulty is that the amplitude of the wrinkles dies off in too singular a fashion, which suggests that we should pick an ansatz from a richer class: we should allow the frequency and amplitude to vary with x_1. It is natural to consider an ansatz of the form

$$v^{(h)}(\boldsymbol{x}) = \lambda(x_1) f(x_1) \sin\left(\frac{x_2}{\lambda(x_1)}\right), \tag{28}$$

so that the amplitude $\lambda(x_1)f(x_1)$ is less singular. Of course, we have to modify Equation (28) to accommodate the boundary conditions $v(x_1, 0) = v(x_1, l) = 0$: in Fourier space, v must have frequencies in a discrete set. As a result, our final ansatz (although motivated by Equation (28)) is slightly different:

$$v^{(h)}(\boldsymbol{x}) = f(x_1) \sum_k \lambda_k \varphi_k(x_1) \sin\left(x_2/\lambda_k\right). \tag{29}$$

Here $\{\varphi_k^2\}$ is a partition of unity. By choosing λ_k and φ_k we can allow the wavelength to vary with x_1. Visually, this is a 'cascade' of wrinkles that get finer and finer near the boundary of the wrinkled zone. Similar constructions have been seen before; see, for example, [20] [6] [15].

4.1 The proof of the upper bound

We prove the upper bound half of Theorem 1.

Proof Our task is to construct an ansatz that wrinkles to waste arc length proportional to $f(x_1)^2$, which was defined in Equation (27).

Step 1: the normal displacement and bending energy. Let $\xi_k = (1 - 4^{-k-1})\xi$ and $\lambda_k = 2^{-k}\lambda_0$. The frequency λ_0 should be approximately $h^{1/3}$, but in order to satisfy the boundary data $v(x_1, l) = 0$ we modify this slightly: $\lambda_0 = \left\lfloor \frac{l}{2\pi h^{1/3}} \right\rfloor^{-1} \frac{l}{2\pi}$. Our interpretation will be that the wrinkles oscillate (in the x_2 direction) with length scale λ_k for $|x_1|$ near ξ_k. The ansatz will only have finitely many frequencies, so we define N_h to be the floor of $-\frac{4}{3}\log_4(h)$.

We take a partition of unity $\left\{\varphi_k^2\right\}_{k=0}^{\infty}$ with φ_k supported on $(-\xi_{k+2}, -\xi_k) \cup (\xi_k, \xi_{k+2})$ if $k > 0$, or $(-\xi_1, \xi_1)$ otherwise. Furthermore, we may and do assume that the derivatives are not needlessly large:

$$|\varphi_k^{(i)}(x_1)| \lesssim (\xi_{k+2} - \xi_k)^{-i} \lesssim 4^{ik} \text{ for } i = 1, 2.$$

We define the vertical displacement:

$$v^{(h)}(\boldsymbol{x}) = f(x_1) \sum_{k=0}^{N_h} \varphi_k(x_1) \lambda_k \sin\left(\frac{x_2}{\lambda_k}\right). \tag{30}$$

For convenience, we define

$$f_k = \begin{cases} \varphi_k f & \text{if } 0 \le k \le N_h \\ 0 & \text{otherwise.} \end{cases} \tag{31}$$

The bounds on the derivatives of φ_k yield the following:

$$\begin{aligned} \sup \left| f_k^{(i)} \right| &\lesssim (\xi - \xi_k)^{1/2-i} \lesssim 2^{(2i-1)k} \text{ for } i = 0, 1, 2, \text{ and} \\ |\operatorname{Spt} f_k| &\le 2(\xi_{k+2} - \xi_k) \lesssim 2^{-2k}, \end{aligned} \tag{32}$$

where the implicit constant in $\lesssim$ does not, of course, depend on k.

We show that $h^2 \int_\Omega \left| \mathbf{B}(v^{(h)}) \right|^2 \mathrm{d}\boldsymbol{x} \lesssim h^{4/3}$, where this quantity is the bending energy of Equation (2). It suffices to show that $\int_\Omega \left| \nabla\nabla v^{(h)} \right|^2 \mathrm{d}\boldsymbol{x} \lesssim h^{-2/3}$. We compute the derivatives of v:

$$\begin{aligned} \partial_1 v^{(h)} &= \sum_{k=0}^{N_h} f_k'(x_1) \lambda_k \sin\left(\frac{x_2}{\lambda_k}\right) \\ \partial_2 v^{(h)} &= \sum_{k=0}^{N_h} f_k(x_1) \cos\left(\frac{x_2}{\lambda_k}\right) \\ \partial_{11} v^{(h)} &= \sum_{k=0}^{N_h} f_k''(x_1) \lambda_k \sin\left(\frac{x_2}{\lambda_k}\right) \\ \partial_{12} v^{(h)} &= \sum_{k=0}^{N_h} f_k'(x_1) \cos\left(\frac{x_2}{\lambda_k}\right) \\ \partial_{22} v^{(h)} &= -\sum_{k=0}^{N_h} f_k(x_1) \lambda_k^{-1} \sin\left(\frac{x_2}{\lambda_k}\right). \end{aligned}$$

By invoking Fourier Isometry with respect to the x_2 variable, we see that

$$\begin{aligned} \int_\Omega \left| \nabla\nabla v^{(h)} \right|^2 \mathrm{d}\boldsymbol{x} &\lesssim \sum_{k=0}^{N_h} \int_{-1/2}^{1/2} (f_k''(x_1))^2 \lambda_k^2 + (f_k'(x_1))^2 + (f_k(x_1))^2 \lambda_k^{-2} \, \mathrm{d}x_1 \\ &\lesssim \sum_{k=0}^{N_h} \left(\sup \left| f_k'' \right|^2 \lambda_k^2 + \sup \left| f_k' \right|^2 + \sup |f_k|^2 \lambda_k^{-2} \right) |\operatorname{Spt} f_k| \\ &\lesssim \sum_{k=0}^{N_h} \left(2^{6k} 2^{-2k} h^{2/3} + 2^{2k} + 2^{-2k} 2^{2k} h^{-2/3} \right) 2^{-2k} \\ &\lesssim 4^{N_h} h^{2/3} + N_h + h^{-2/3} \lesssim h^{-2/3} \end{aligned}$$

because we chose N_h such that $4^{N_h} \le h^{-4/3}$.

Step 2: the tangential displacement and the membrane energy. We must define $\boldsymbol{u}^{(h)}$ and show that the membrane energy is controlled by $\mathcal{E}_0 + C' h^{4/3}$. This comes from three physical effects:

- The outer edges $\{|x_1| > \xi\}$ are stretched vertically, which results in exactly $\mathcal{E}_0$ energy.
- The wrinkles would waste *exactly* the right arc length if we took $N_h = \infty$. However, that would cost infinite bending energy. Our failure to match the relaxed energy will contribute $o(h^{4/3})$ energy.
- The wrinkles cannot be isometric. This contributes $O(h^{4/3})$ energy.

The membrane energy consists of three summands, which represent horizontal stretching (m_{11}), shearing (m_{12}), and vertical stretching (m_{22}):

$$\int_\Omega |\mathbf{M}(\boldsymbol{u}, v)|^2 \,\mathrm{d}\boldsymbol{x} = \int_\Omega \left(m_{11}^2 + 2m_{12}^2 + m_{22}^2\right) \mathrm{d}\boldsymbol{x}.$$

Instead of opening with a definition of $\boldsymbol{u}^{(h)}$ and checking each of these terms afterwards, we will first define $u_2^{(h)}$ to make $m_{22} = 0$ sufficiently far inside the wrinkled zone, then define $u_1^{(h)}$ so that $m_{12} = 0$. The ansatz will then be complete, so we will need only to check that m_{11} is sufficiently small.

Step 2a: vertical stretching. Let $\psi(x_1) = \sum_{k=0}^{N_h} \varphi_k^2(x_1)$. We note that $\psi(x_1) = 1$ for $|x_1| < \xi_{N_h}$, $\psi(x_1) = 0$ for $|x_1| > \xi_{N_h+2}$, and that it is between 0 and 1 for intermediate values of x_1.

From Equation (3), we recall that $m_{22} = \partial_2 u_2 + \frac{1}{2}\left(\partial_2 v + \omega x_1\right)^2 - \frac{1}{2}\omega^2\xi^2$. We let

$$\begin{aligned} \partial_2 u_2^{(h)} &= -\frac{1}{2}\left((\partial_2 v^{(h)})^2 - \frac{1}{2}f^2\psi\right) - \omega x_1 \partial_2 v^{(h)} \\ &:= -\frac{1}{2}\vartheta^{(h)}(\boldsymbol{x}) - \omega x_1 \partial_2 v^{(h)}. \end{aligned} \tag{33}$$

In principle we should check that $u_2^{(h)}$ satisfies the boundary conditions of Theorem 1. We delay this until Step 2b and compute the vertical strain:

$$\begin{aligned} m_{22}(\boldsymbol{u}^{(h)}, v^{(h)}) &= \partial_2 u_2^{(h)} + \frac{1}{2}\left(\left(\partial_2 v^{(h)}\right)^2 - \frac{1}{2}f^2\right) + \omega x_1 \partial_2 v^{(h)} + \frac{1}{2}\omega^2(x_1^2 - \xi^2)_+ \\ &= -\frac{1}{4}f^2(x_1)\left(1 - \psi(x_1)\right) + \frac{1}{2}\omega^2(x_1^2 - \xi^2)_+. \end{aligned}$$

Notice that the first term vanishes in $\{|x_1| > \xi\}$, and the second in $\{|x_1| < \xi\}$. Using this and the definition $E^{(0)}(\mathbf{0}, 0) = \mathcal{E}_0$ (Equation 8), the energy from vertical stretching is

$$\int_\Omega m_{22}^2(\boldsymbol{u}^{(h)}, v^{(h)}) \,\mathrm{d}\boldsymbol{x} = \frac{1}{16}\int_\Omega f^4(x_1)\left(1 - \psi(x_1)\right)^2 \mathrm{d}\boldsymbol{x} + \mathcal{E}_0.$$

The integrand is even in x_1 and supported on a narrow strip near the edges $x_1 = \pm\xi$, so

$$\int_\Omega m_{22}^2(\boldsymbol{u}^{(h)}, v^{(h)}) \,\mathrm{d}\boldsymbol{x} - \mathcal{E}_0 \lesssim \int_{\xi - \xi_{N_h}}^{\xi} f^4(x_1) \,\mathrm{d}x_1 \lesssim (\xi - \xi_{N_h})^3 \lesssim h^4.$$

As promised, this term is much smaller than $h^{4/3}$.

Step 2b: the shear energy and boundary data on $\boldsymbol{u}^{(h)}$. In the statement of the theorem we insisted that u_2 be 0 at the top $x_2 = l$ and bottom $x_2 = 0$. We must therefore check that the proposed $\partial_2 u_2$ integrates to 0 is x_2, for any fixed x_1. This follows immediately from the fact that $\vartheta^{(h)}$ is mean-0 in x_2, or from the following computation:

$$\begin{aligned}
\vartheta^{(h)} &= \left(\sum_{k=0}^{N_h} f\varphi_k \cos\left(\frac{x_2}{\lambda_k}\right)\right)^2 - \frac{1}{2}f^2 \sum_{k=0}^{N_h} \varphi_k^2 \\
&= \sum_{k=0}^{N_h} f_k^2 \left(\cos^2\left(\frac{x_2}{\lambda_k}\right) - \frac{1}{2}\right) + 2f_k f_{k+1} \cos\left(\frac{x_2}{\lambda_k}\right)\cos\left(\frac{x_2}{\lambda_{k+1}}\right) \\
&= \sum_{k=0}^{N_h} \frac{1}{2} f_k^2 \cos\left(\frac{2x_2}{\lambda_k}\right) + f_k f_{k+1}\left(\cos\left(\frac{3x_2}{\lambda_k}\right) + \cos\left(\frac{x_2}{\lambda_k}\right)\right). \qquad (34)
\end{aligned}$$

Writing down the exact solution will become cumbersome, so instead we note that $\vartheta^{(h)}$ is of the following form:

$$\vartheta^{(h)} = \sum_k \sum_{j=1}^{3} \alpha_j f_k^2 \cos\left(\frac{jx_2}{\lambda_k}\right) + \beta_j f_k f_{k+1} \cos\left(\frac{jx_2}{\lambda_k}\right),$$

for coefficients α_j, β_j which depend on nothing execpt j. In particular, they do not depend on h. [11]

We pick $u_1^{(h)}$ such that the shear strain m_{12} vanishes:

$$\begin{aligned}
\partial_2 u_1^{(h)} &= -\partial_1 u_2^{(h)} - \omega x_1 \partial_1 v^{(h)} + \omega v^{(h)} - \partial_1 v^{(h)} \partial_2 v^{(h)} \\
&= \frac{1}{2}\partial_1 \int \vartheta^{(h)}\, \mathrm{d}x_2 + \omega \partial_1 (x_1 v^{(h)}) \\
&\quad - \omega x_1 \partial_1 v^{(h)} + \omega v^{(h)} - \sum_{k=0}^{N_h} f_k \cos\left(\frac{x_2}{\lambda_k}\right) \sum_{l=0}^{N_h} \lambda_l f_l' \sin\left(\frac{x_2}{\lambda_l}\right) \\
&= \frac{1}{2}\partial_1 \int \vartheta^{(h)}\, \mathrm{d}x_2 + 2\omega v^{(h)} - \sum_{k=0}^{N_h} f_k \cos\left(\frac{x_2}{\lambda_k}\right) \sum_{l=0}^{N_h} \lambda_l f_l' \sin\left(\frac{x_2}{\lambda_l}\right)
\end{aligned}$$

This expression is of the form

$$\begin{aligned}
\partial_2 u_1^{(h)} = 2\omega v^{(h)} &+ \sum_k \lambda_k \sum_{j=1}^{3} \alpha_j f_k f_k' \sin\left(\frac{jx_2}{\lambda_k}\right) \qquad (35) \\
&+ \sum_k \lambda_k \sum_{j=1}^{3} \beta_j f_k' f_{k+1} \sin\left(\frac{jx_2}{\lambda_k}\right) + \gamma_j f_k f_{k+1}' \sin\left(\frac{jx_2}{\lambda_k}\right)
\end{aligned}$$

for different constants α_j, β_j and γ_j. Note that $\partial_2 u_1^{(h)}$ still integrates to 0 in the x_2 direction, so it is consistent with the boundary condition that $u_1^{(h)}(\boldsymbol{x}) = 0$ at $x_1 = 0$ and l.

[11] There is no 'off by one' error at the upper limit of the summation: recall from Equation (31) that $f_{N_h+1} = 0$.

Step 2c: stretching energy along the wrinkles. The final term in the strain matrix is

$$m_{11} = \partial_1 u_1^{(h)} + \frac{1}{2}\left(\partial_1 v^{(h)}\right)^2. \tag{36}$$

We bound $\int_\Omega \left|\partial_1 u_1^{(h)}\right|^2 \mathrm{d}\boldsymbol{x}$ and $\int_\Omega \left(\partial_1 v^{(h)}\right)^4 \mathrm{d}\boldsymbol{x}$ separately.

We first show that $\int_\Omega \left|\partial_1 u_1^{(h)}\right|^2 \mathrm{d}\boldsymbol{x} \lesssim h^{4/3}$.

To find $\partial_1 u_1^{(h)}$, we take the general form of $\partial_2 u_1^{(h)}$ (Equation 35) and integrate once in x_2 while differentiating in x_1. The integration in x_2 helps: it gives us a factor of $\lambda_k \approx 2^{-k} h^{1/3}$ in the summation, which is small in h *and* helps the summand converge. The derivative in x_1 hurts: by Equation (32), we see that taking derivatives in x_1 makes the summand more singular. The following computation has two purposes: we show that $\partial_1 u_1^{(h)}$ scales as $h^{2/3}$, and that the summation converges.

From Equation (35), we see that

$$\begin{aligned}\partial_1 u_1^{(h)} = 2\omega \sum_k \lambda_k^2 f_k' \cos\left(\frac{x_2}{\lambda_k}\right) \\ + \sum_k \lambda_k^2 \sum_{j=1}^{3}\sum_{l=0}^{2}\left[\alpha_{j,l} f_k^{(l)} f_k^{(2-l)} \cos\left(\frac{j x_2}{\lambda_k}\right) + \beta_{j,l} f_k^{(l)} f_{k+1}^{(2-l)} \cos\left(\frac{j x_2}{\lambda_k}\right)\right],\end{aligned} \tag{37}$$

where again the coefficients do not depend on anything except j and l. By Parseval's Theorem,

$$\begin{aligned}\left\|\partial_1 u_1^{(h)}\right\|_{L^2}^2 &\lesssim \sum_{k=0}^{N_h} \lambda_k^4 \|f_k'\|_{L^2}^2 + \sum_k \sum_{l=0}^{2} \lambda_k^4 \left[\|f_k^{(l)} f_k^{(2-l)}\|_{L^2}^2 + \|f_k^{(l)} f_{k+1}^{(2-l)}\|_{L^2}^2\right] \\ &\le \sum_{k=0}^{N_h} \lambda_k^4 \left|\operatorname{Spt} f_k\right| \left\|f_k'\right\|_{L^\infty}^2 + \sum_k \sum_{l=0}^{2} \lambda_k^4 \left|\operatorname{Spt} f_k\right| \left\|f_k^{(l)}\right\|_{L^\infty}^2 \left\|f_k^{(2-l)}\right\|_{L^\infty}^2 \\ &\quad + \sum_k \sum_{l=0}^{2} \lambda_k^4 \left|\operatorname{Spt} f_k \cap \operatorname{Spt} f_{k+1}\right| \left\|f_k^{(l)}\right\|_{L^\infty}^2 \left\|f_{k+1}^{(2-l)}\right\|_{L^\infty}^2 \\ &\lesssim \sum_k \lambda_k^4 \left|\operatorname{Spt} f_k\right| \left[\|f_k'\|_{L^\infty}^2 + \|f_k'\|_{L^\infty}^4 + \|f_k\|_{L^\infty}^2 \|f_k''\|_{L^\infty}^2\right] \\ &\lesssim \sum_k \lambda_0^4\, 2^{-4k} 2^{-2k} \left[2^{2k} + 2^{4k} + 2^{-2k} 2^{6k}\right] \lesssim \lambda_0^4.\end{aligned}$$

We found the penultimate line by using AM-GM to separate $\|f_k\|_{L^\infty}$ and $\|f_{k+1}\|_{L^\infty}$, then group like terms. Note that λ_{k+1} differs from λ_k by a multiplicative constant. The last line follows from Equation (32). Finally, we note that we have chosen λ_0 to be approximately $h^{1/3}$, so as promised this proves that $\int_\Omega \left|\partial_1 u_1^{(h)}\right|^2 \mathrm{d}\boldsymbol{x} \lesssim h^{4/3}$.

We show that $\int_\Omega \left(\partial_1 v^{(h)}\right)^4 \mathrm{d}\boldsymbol{x} \lesssim h^{4/3}$, which concludes step 2c and the proof. We start by invoking Parseval's Theorem with respect to x_2:

$$\int_\Omega \left(\partial_1 v^{(h)}\right)^4 \mathrm{d}\boldsymbol{x} = \int_{-1/2}^{1/2} \left\|\left(\partial_1 v^{(h)}(x_1, \cdot)\right)^2\right\|_{L^2}^2 \mathrm{d}x_1 = \sum_j \int a_j^2(x_1)\, \mathrm{d}x_1, \tag{38}$$

where the a_j are the Fourier coefficients of $\left(\partial_1 v^{(h)}\right)^2$. Our expression for $v^{(h)}$ is already in the form of a Fourier Series:

$$\begin{aligned}\left(\partial_1 v^{(h)}\right)^2 &= \left(\sum_k \lambda_k f_k' \sin\left(\frac{x_2}{\lambda_k}\right)\right)^2 \\ &= \sum_k \lambda_k^2 (f_k')^2 \sin^2\left(\frac{x_2}{\lambda_k}\right) + 2\lambda_k\lambda_{k+1} f_k' f_{k+1}' \sin\left(\frac{x_2}{\lambda_k}\right)\sin\left(\frac{x_2}{\lambda_{k+1}}\right) \\ &= \sum_k \frac{\lambda_k^2}{2}(f_k')^2\left(1-\cos\left(\frac{2x_2}{\lambda_k}\right)\right) \\ &\quad + \lambda_k\lambda_{k+1} f_k' f_{k+1}'\left(\cos\left(\frac{x_2}{\lambda_k}\right) - \cos\left(\frac{3x_2}{\lambda_k}\right)\right).\end{aligned}$$

We write the above expression as $\sum_j a_j \cos(2\pi j x_2/l)$, then use that $\left|f_k' f_{k+1}'\right| \le \frac{1}{2}\left((f_k')^2 + (f_{k+1}')^2\right)$ to conclude that

$$\int \sum_j a_j^2 \,\mathrm{d}x_1 \lesssim \sum_k \lambda_k^4 \int (f_k')^4 \,\mathrm{d}x_1 \lesssim \sum_k \lambda_0^4 2^{-4k} 2^{4k} 4^{-k} \lesssim \lambda_0^4.$$

By the above and Equation (38), $\int_\Omega \left(\partial_1 v^{(h)}\right)^4 \mathrm{d}\boldsymbol{x} \lesssim h^{4/3}$.

In the preceding construction, the wavelength of the wrinkles varies with x_1; this is sometimes called a "cascade of wrinkles." There are experimental settings where a cascade of wrinkles is observed [1] [18] [29] [7]. However, we are not aware of any experimental evidence that a twisted ribbon exhibits a cascade of wrinkles. This does not contradict the present result: the energy-minimizing configuration might look quite different, to the eye, than our ansatz. In particular, we expect that there are other ways of evading the difficulty encountered in Example 1. For any v, if we take the Fourier transform of v with respect to x_2 alone, we get an expression that resembles Equation (29):

$$v(\boldsymbol{x}) = \sum_m \hat{a}_m(x_1) \sin\left(\frac{2m\pi}{l} x_2\right).$$

A cascade of wrinkles can be seen as a special case of this, where (for fixed x_1) only two frequencies are present. We need to emphasize higher frequencies for x_1 closer to the edge $\pm\xi$, but there are many ways of doing that and we used only two frequencies solely for convenience.

References

1. Ali S. Argon, Vijay Gupta, H. S. Landis, and James A. Cornie. Intrinsic toughness of interfaces between SiC coatings and substrates of Si or C fibre. *Journal of Materials Science*, 24(4):1207–1218, 1989.
2. Basile Audoly and Yves Pomeau. *Elasticity and geometry : from hair curls to the non-linear response of shells*. Oxford University Press, Oxford, New York, Auckland, 2010. Autre tirage : 2011.

3. Jean-François Babadjian. Traces of functions of bounded deformation. *Indiana University Mathematics Journal*, 64:1271–1290, 2015.
4. Jacob Bedrossian and Robert V. Kohn. Blister patterns and energy minimization in compressed thin films on compliant substrates. *Communications on Pure and Applied Mathematics*, 68(3):472–510, 2015.
5. Peter Bella and Robert V. Kohn. Metric-induced wrinkling of a thin elastic sheet. *Journal of Nonlinear Science.*, 24(6):1147–1176, 2014.
6. Peter Bella and Robert V. Kohn. Wrinkles as the result of compressive stresses in an annular thin film. *Communications on Pure and Applied Mathematics*, 67(5):693–747, 2014.
7. Peter Bella and Robert V. Kohn. Coarsening of folds in hanging drapes. *Communications on Pure and Applied Mathematics*, 70(5):978–1021, 2017.
8. H. Ben Belgacem, Sergio Conti, Antonio DeSimone, and Stefan Müller. Rigorous bounds for the Föppl-von Kármán theory of isotropically compressed plates. *Journal of Nonlinear Science*, 10(6):661–685, Dec 2000.
9. E. Cerda and L. Mahadevan. Geometry and physics of wrinkling. *Physical Review Letters*, 90:074302, Feb 2003.
10. Julien Chopin, Vincent Démery, and Benny Davidovitch. Roadmap to the morphological instabilities of a stretched twisted ribbon. *Journal of Elasticity*, 119(1-2):137–189, 2015.
11. Julien Chopin and Arshad Kudrolli. Helicoids, wrinkles, and loops in twisted ribbons. *Physical Review Letters*, 111:174302, Oct 2013.
12. Philippe G. Ciarlet. A justification of the von Kármán equations. *Archive for Rational Mechanics and Analysis*, 73(4):349–389, Dec 1980.
13. Sergio Conti, Francesco Maggi, and Stefan Müller. Rigorous derivation of Föppl's theory for clamped elastic membranes leads to relaxation. *SIAM Journal on Mathematical Analysis*, 38(2):657–680, 2006.
14. Bernard Dacorogna. *Direct Methods in the Calculus of Variations.* Applied Mathematical Sciences. Springer New York, 2 edition, 2007.
15. Benny Davidovitch. Period fissioning and other instabilities of stressed elastic membranes. *Physical Review E*, 80:025202, Aug 2009.
16. Gero Friesecke, Richard D James, and Stefan Müller. The Föppl-von Kármán plate theory as a low energy Γ-limit of nonlinear elasticity. *Comptes Rendus Mathematique*, 335(2):201 – 206, 2002.
17. John Gemmer, Eran Sharon, Toby Shearman, and Shankar C. Venkataramani. Isometric immersions, energy minimization and self-similar buckling in non-Euclidean elastic sheets. *Europhysics Letters*, 114(2), 4 2016.
18. Gustavo Gioia and Michael Ortiz. Delamination of compressed thin films. *Advances in Applied Mechanics*, 33:119–192, 1997.
19. Albert E. Green. The elastic stability of a thin twisted strip. II. *Proceedings of the Royal Society of London. Series A, Mathematical and Physical Sciences*, 161(905):197–220, 1937.
20. Weimin Jin and Peter Sternberg. Energy estimates for the von Kármán model of thin-film blistering. *Journal of Mathematical Physics*, 42(1):192–199, 2001.
21. Robert V. Kohn. Energy-driven pattern formation. *Proceedings of the International Congress of Mathematicians*, 1:359–383, 2006.
22. Robert V. Kohn and Hoai-Minh Nguyen. Analysis of a compressed thin film bonded to a compliant substrate: The energy scaling law. *Journal of Nonlinear Science*, 23(3):343–362, Jun 2013.

23. Joseph D. Paulsen, Evan Hohlfeld, Hunter King, Jiangshui Huang, Zhanlong Qiu, Thomas P. Russell, Narayanan Menon, Dominic Vella, and Benny Davidovitch. Curvature-induced stiffness and the spatial variation of wavelength in wrinkled sheets. *Proceedings of the National Academy of Sciences*, 113(5):1144–1149, 2016.
24. Huy Pham Dinh, Vincent Démery, Benny Davidovitch, Fabian Brau, and Pascal Damman. From cylindrical to stretching ridges and wrinkles in twisted ribbons. *Physical Review Letters*, 117:104301, Sep 2016.
25. Allen C. Pipkin. The relaxed energy density for isotropic elastic membranes. *IMA Journal of Applied Mathematics (Institute of Mathematics and Its Applications)*, 36(1):85–99, 1986.
26. Monty J. Strauss. Variations of Korn's and Sobolev's equalities. *Proceedings of Symposia in Pure Mathematics*, 23:207214, 1973.
27. Matteo Taffetani and Dominic Vella. Regimes of wrinkling in pressurized elastic shells. *Philosophical Transactions of the Royal Society of London A: Mathematical, Physical and Engineering Sciences*, 375(2093), 2017.
28. Roger Temam and Gilbert Strang. Functions of bounded deformation. *Archive for Rational Mechanics and Analysis*, 75(1):7–21, 1980.
29. Hugues Vandeparre, Miguel Piñeirua, Fabian Brau, Benoit Roman, José Bico, Cyprien Gay, Wenzhong Bao, Chun Ning Lau, Pedro M. Reis, and Pascal Damman. Wrinkling hierarchy in constrained thin sheets from suspended graphene to curtains. *Physical Review Letters*, 106:224301, Jun 2011.
30. Thomas A. Witten. Stress focusing in elastic sheets. *Reviews of Modern Physics*, 79:643–675, Apr 2007.